

# A Modular Custom Aperture Technology for Optimization of MEMS Scanners

Daniel T. McCormick, Veljko Milanović and Kenneth Castelino

Adriatic Research Institute  
Berkeley, CA 94706

In this work a MEMS based, customizable aperture size, beam steering technology is demonstrated. Sets of electrostatic actuators optimized for speed, angle, area footprint or resonant driving are designed and realized in a self-aligned DRIE fabrication process. Metallized, low-inertia, thinned single crystal silicon mirrors stiffened by a backbone of thicker silicon beams are created in a separate fabrication process. The diameter, as well as geometry, of the mirror is selected, and paired with an actuator, in order to optimize the trade-offs between speed, beam size and scan angle for each individual application. The mirrors are subsequently bonded to the actuators. By partially decoupling the design of the actuators and apertures a wider set of parameter trade offs become available. The modular approach allows either the absolute optimization of a device prior to fabrication, or the ability to economically adapt a small set of fabricated devices for a wide range of applications. This is common in galvanometer based large-scale systems, but has not previously been available in MEMS technologies.

Scanning mirrors exhibiting fast point-to-point, or resonant, scanning speeds and high resolution are critical elements in a diverse range of application areas including: optical communications, medical imaging, adaptive optics, LIDAR systems and displays. Each application has a unique set of design specifications based on performance requirements. In most cases, designers trade off among three primary parameters: speed, aperture size, and angle. A given set of design trade offs may be possible in a specialized MEMS technology, however, this same set of trade offs will most likely not satisfy the requirements for other applications. A modular approach to MEMS scanner design is required in order to effectively address this problem. Namely, the system designer would ideally want to choose from a set of available actuators and mirrors to attain a desired parameter space for their application.

In this study, three types of gimbal-less two-axis actuator designs are employed. The previously presented<sup>1</sup> gimbal-less two-axis actuators, realized in the multilevel beam SOI-MEMS fabrication process,<sup>2</sup> lend themselves inherently to a modular design approach, and are therefore employed in the present work. Namely, each actuator can utilize rotating vertical combdrives of arbitrary length, arbitrarily stiff linkages, and arbitrarily positioned mechanical rotation transformer linkages. A schematic diagram presenting the conceptual operation of the gimbal-less 2D designs is shown in Fig 1. The three device types are: *B-type*, *L-type* and *M-type*. The *B* device is designed to operate at low voltages (10° mechanical at 119V), exhibit the largest scan angle (18.2° mechanical at 160V) and occupy a small die size (3mm×3mm) with a resonant frequency of 3.72kHz. The *L* devices operate at higher voltages (10° mechanical at 143V) and obtain higher scanning speeds with reduced angle (13.4° maximum,  $f_r = 5.44\text{kHz}$ ) while occupying a die size of 3.1mm×3.1mm. Finally, the *M* device requires the highest driving voltages (10° mechanical at 145V) and a larger die size (5.1mm×5.1mm) in order to provide the fastest scanning speeds (8.04kHz).<sup>\*</sup> SEMs of the *M* and *L* actuator design are provided in Fig 2.

The mirrors are fabricated on a separate SOI wafer. The thickness of the SOI device layer is chosen based on the required stand-off distance between the mirror and the actuator (i.e. the pedestal height), and the thickness of the mirror plate. The pedestal height must be sufficient to allow the mirror to deflect the required angle when both axes are activated (15° mechanical). The presented mirrors are realized with a 120 $\mu\text{m}$  device layer thickness. In the first step of the fabrication process a thick thermal oxide layer (2 $\mu\text{m}$ ) is grown. The oxide is then patterned employing three consecutive lithography steps and RIE oxide etches. This results in multilevel oxide hardmask for subsequent DRIE silicon etches. During the first DRIE step only the areas which will be fully etched to the buried oxide layer are exposed; the first etch is performed to a depth significantly greater than the final thickness of the mirror. A blanket oxide RIE then removes the thinnest oxide hardmask, and thins the remaining oxide hardmasks. The second DRIE etch defines the thickness of the trusses by recessing the mirror plate. The next oxide RIE removes the truss mask. The final frontside DRIE lowers the perimeter trenches as well as the mirror and trusses until trenches reach the buried oxide layer and the desired mirror plate thickness is reached. Following the completion of the frontside etches the backside of the wafer is etched, creating openings to expose the mirror surfaces. In the final process step, the oxide layer on the mirror surfaces is removed in a hydrofluoric wet etch and the mirrors, still attached to the SOI wafer by tethers, are metalized on both sides. A process separating the fabrication of the trussed mirrors and pedestals is also available if precise, ultra-thin (sub 2 $\mu\text{m}$ ) mirrors are required. An overview of the mirror fabrication process is presented in Fig 3, and SEMs of various mirrors are provided in Fig 4; images of bonded actuators and mirrors are shown in Fig 5.

The multi-level process allows a thinned mirror plate (1.5 $\mu\text{m}$  to 15 $\mu\text{m}$ ) to be created with a tall pedestal and a backbone or skeleton formed by thicker trusses to provide both low inertia, i.e. a high resonant frequency, and stiffness to minimize curvature after metalization as well as dynamic deformation. Apertures as large as 2mm have been fabricated and characterized, a summary of theoretical and experimental results is provided in Fig 6.

---

<sup>\*</sup>The resonant frequencies are given for a 0.8mm diameter aperture.

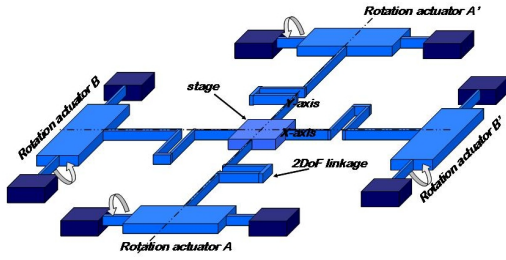


**Figure 1.** A schematic diagram of the gimbal-less actuator structure; the motion of the  $x$  and  $y$  axis are decoupled via the looped spring design and both axis may operate at high frequencies.

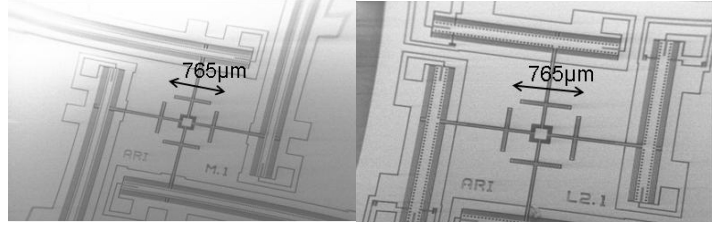


**Figure 2.** SEMs of designed and fabricated actuators; the device on the *left* is optimized for the highest scanning speed while the device of the *right* achieves larger angles while occupying a smaller die area.

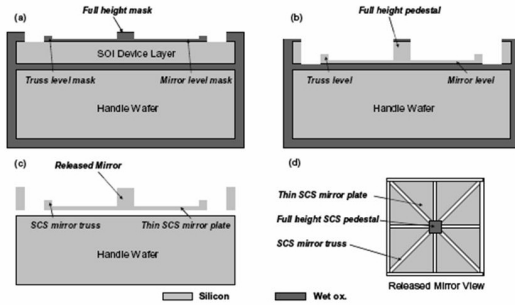


**Figure 3.** An overview of the mirror fabrication process. The thickness of the pedestal, trusses and mirror plate as well as the reflective coating, mirror geometry and diameter may be optimized for a specific application.

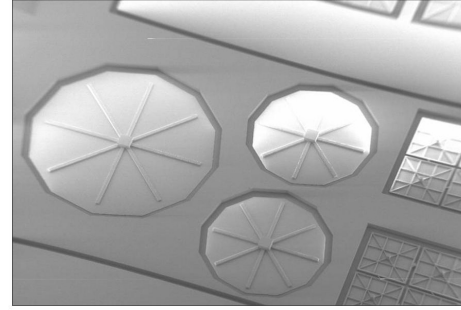


**Figure 4.** SEMs of various fabricated mirrors, with a  $1.5\mu\text{m}$  thick mirror plate; nominal mirror diameters are between  $500\mu\text{m}$  and  $1.2\text{mm}$ ; mirrors as large as  $1.6\text{mm}$  and  $2.0\text{mm}$  have been fabricated, bonded to actuators and tested.

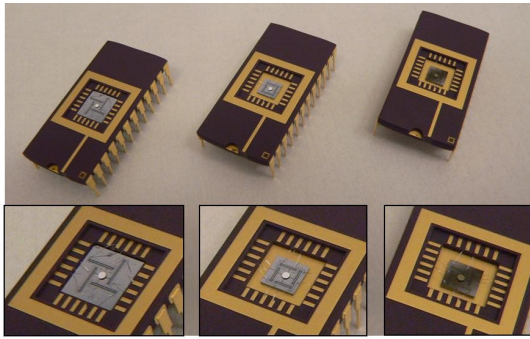


**Figure 5.** Optical images of various metalized mirrors bonded to different actuators in standard 24 pin DIP packages.

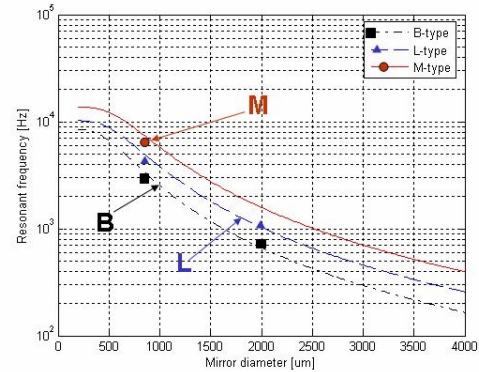


**Figure 6.** A plot of theoretical and measured scanner frequency as a function of bonded mirror diameter.

## ACKNOWLEDGMENTS

The authors would like to acknowledge and thank Dr. Chris Keller of MEMSPI for providing the micro-tools utilized in this work.

## REFERENCES

1. V. Milanonovic, D. McCormick, and G. Matus, "Gimbal-less monolithic silicon actuators for tip-tilt-piston micromirror applications," *IEEE J. of Select Topics in Quantum Electronics* **10**, pp. 462–471, 2004.
2. V. Milanonovic, "Multilevel-beam soi-mems fabrication and applications," *IEEE/ASME Journal of Microelectromechanical Systems* **13**, pp. 19–30, 2004.

Daniel T. McCormick- email: dmcc@adriaticresearch.org  
828 San Pablo Ave., Suite 115E, Berkeley, CA 94706